

Study of the Ag^+ Hydration by Means of a Semicontinuum Quantum-Chemical Solvation Model

José M. Martínez, Rafael R. Pappalardo, and Enrique Sánchez Marcos*[†]

Departamento de Química Física, Facultad de Química, Universidad de Sevilla, 41012-Sevilla, Spain

Received: January 8, 1997; In Final Form: April 3, 1997[⊗]

The changes in the distance between the cation and the oxygen of the first water shell ($\text{M}-\text{O}_1$) induced by the rest of the solvent and the hydration structure of Ag^+ have been theoretically studied using a mixed discrete-continuum model of solvation. Ab initio calculations at the MP2 level for $[\text{Ag}(\text{H}_2\text{O})_n]^+$ clusters ($n = 1, 2, 4,$ and 12 , the last one formed by two water shells ($4 + 8$)) in gas phase and solution were carried out with DZ+ polarization basis sets and Stevens et al.'s pseudopotentials. The bulk solvent was simulated by means of Nancy's group continuum solvation model. The clusters were placed in a cavity surrounded by a continuum with the static dielectric permittivity of the water. Geometry optimization was performed in all cases. Calculations allow the examination of the specific interaction effects on the first solvation shell due to the hydrogen-bonded water molecules of the second shell as well as the long-range interactions of the bulk solvent, described as a dielectric continuum. Likewise, the combination of both effects is studied by the explicit consideration of a Ag^+ polyhydrate containing two hydration shells, $[\text{Ag}(\text{H}_2\text{O})_{12}]^+$, immersed in a cavity. Opposite effects on the $\text{Ag}-\text{O}_1$ distance were observed by the specific and long-range (continuum) solvent interactions. Specific interactions, mainly hydrogen bonding, shorten the bond, whereas long-range interactions lengthen it, leading to a mutual partial cancellation of the effects when the two types of interactions are jointly considered. Contributions to the Ag^+ hydration enthalpy have also been examined in terms of the semicontinuum model.

1. Introduction

The structure and dynamics of hydrated ions has long been an important topic in chemical physics and biochemistry. There is a large number of physicochemical phenomena and technical processes in solution where these species are involved. They play either a central role, as in many electron transfer processes or enzymatic reactions, or a secondary role, as in the salting effect or the flocculation of colloid particles.^{1,2} Since the earliest theories, the ionic radius was an important concept to deal with thermodynamic, transport, spectroscopic, and reactivity properties of electrolytes,³ although this magnitude is not an observable. Marcus in a recent review on this subject⁴ shows that the primary source of information for ionic radii is the interparticle distance. A large number of data from both experimental techniques (X-ray and neutron scattering, and EXAFS) and computer simulations (Monte Carlo and molecular dynamics) have been collected mainly during the past three decades. Excellent compilations can be found in the reviews of Marcus⁴ and Ohtaki and Radnai⁵ and the book of Magini et al.⁶ Quantum chemical studies of hydrated ions have also been useful for understanding solvated systems and in determining nonempirical intermolecular potentials or related properties involved in the statistical simulations of the solutions.⁷ Thus, the first estimate of the ion–water distance uses to come from quantum-mechanical calculations where the structure of a $\text{M}^{m+}(\text{H}_2\text{O})_n$ or $\text{A}^{1-}(\text{H}_2\text{O})_x$ cluster is optimized.³ However, comparison of the structural parameters obtained from these calculations with the experimental ones needs the explicit consideration of the surrounding solvent which completes the condensed medium. Quantum-chemical models of solvation via either the discrete or the continuum approach have been used to investigate such solvent effects.⁸ Different authors have examined the change

of the $R(\text{M}-\text{O}_1)$ distance induced by the inclusion of one or several water molecules coordinated to the hydrated cluster, which represents partially the effect of a second shell. The specific interactions associated to the second hydration shell are dominated by the hydrogen-bonded medium and lead to a decrease of the $R(\text{M}-\text{O}_1)$ distance.^{9–11} On the contrary, we had shown that when the hydrated ion is relaxed within a cavity embedded in a dielectric continuum, the long-range solute–solvent interactions lead to an increase of the $R(\text{M}-\text{O}_1)$ distance.¹² Tuñón et al.¹³ find the same behavior of the continuum approach in the solvation study of the H_3O^+ cation. These opposite trends of the supermolecule and continuum models are well understood on the basis of both approaches. In the discrete description the first-shell water molecules become more polarized when they get closer to the central cation. As a consequence, hydrogen bonds with water molecules of the second hydration shell are stronger.¹⁴ In the continuum model the interaction of the solute with the solvent reaction field is enhanced with the augmentation of the intermolecular distances. This is a consequence of the increase of solute's multipoles which interact with the solvent reaction field, as has been shown by several authors.^{15,16}

The representation of the solvent by means of a dielectric continuum eliminates detailed structural properties of the solution which are important in polar and protic solvents, such as water.¹⁷ In this sense, this model may be envisaged as a crude approximation for the solvation model. Nevertheless, its intrinsic simplicity allows an easy way to include the extremely important long range solute–solvent interactions within the quantum Hamiltonian of a solute. This facilitates the consideration of solvent effects on solute's properties as a standard option available to quantum chemists.^{18–20} On the contrary, a discrete approach of the solvent should need a number of individual solvent particles much greater than that computationally accessible not only at the quantum chemical level but

[†] E-mail: sanchez@mozart.us.es.

[⊗] Abstract published in *Advance ACS Abstracts*, May 15, 1997.

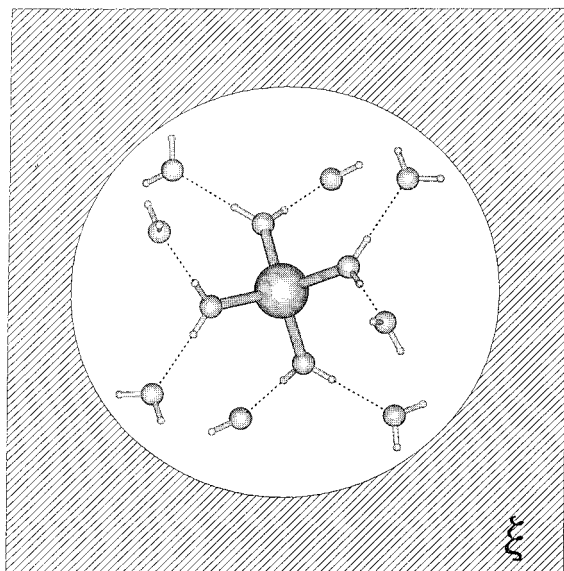


Figure 1. Schematic representation of the semicontinuum model of solvation including two discrete hydration shells and a continuum one.

also at the statistical simulation one.^{21,22} Thus, to attain correct description of ionic or polar solute solutions by simulation techniques, methods such as the Ewald sum or the reaction field have to be included.²³ Therefore, a semicontinuum model seems to be an equilibrated approach to the problem. In this work, the modelization is completely performed within a quantum-mechanical framework, but interesting alternatives based on hybrid quantum mechanics/classical mechanics formalism can also be employed.²⁴

As far as the hydration of metallic cation is concerned, both Tuñón et al.¹³ and Akesson et al.²⁵ have pointed out that the use of a mixed discrete-continuum model considering explicitly the first hydration shell is not sufficient to fulfill the requirement of the surrounding hydrogen-bonded medium and the charge-transfer process to the outer shells. The aim of this work is to extend our previous study on the hydration of metallic cations¹² in the way suggested by the above-mentioned authors in order to clarify which is the global behavior when both factors hydrogen bonding and long-range interactions are simultaneously considered. A semicontinuum quantum-chemical model (Figure 1), where the hydrated ion is surrounded by a second shell of quantum-mechanically described water molecules has been used. The whole cluster is immersed in a cavity embedded in a dielectric continuum, which represents the bulk solvent. For the present study, we have selected the silver cation, which it is accepted to have a first-shell hydration number of 4,^{26,27} which reduces to 12 the number of water molecules to be explicitly considered in the two hydration shells. The fact that Ag⁺ is a soft monovalent cation prevents the solute-solvent electrostatic interactions from concealing other weaker interactions. In this sense, geometrical relaxation of the Ag-O_I distances under solvent perturbation should be significant.

2. Methodology

MP2 calculations of the hydrated ion [Ag(H₂O)_{*n*}]⁺ for *n* = 1, 2, 4, and 12 have been carried out using Stevens et al.'s pseudopotentials for Ag and O and double-zeta-polarization (DZP) basis sets.²⁸ Several tests with different basis sets on the dihydrate were performed to estimate the order of magnitude of the BSSE, obtaining for the basis sets selected values around 4 kJ/mol, which are to be compared with a total interaction energy of around 100 kJ/mol. The small error found, the partial cancellation of it, given our comparative goal, and the controversy about to what extent BSSE corrections improve the

reliability of the results^{11,29} compelled us not to include such corrections in our study. To test the effects of more extended basis sets on the interaction energies, single-point calculations on the optimized structures have been carried out with Ag basis sets supplemented with (spf) functions ($\xi_s = 0.0294$, $\xi_p = 0.0195$, $\xi_f = 1.5000$),³⁰ such that TZP quality is reached for Ag⁺, and for H and O atoms, the corresponding 6-311G** basis sets are used. The MP2 interaction energies computed with BSSE correction do not alter significantly the values presented below. Full geometry optimization in gas phase and within the cavity was performed for the clusters with *n* = 1, 2, and 4. When the first shell was completed, the Ag-O_I distances were optimized at the same value, so that the possibility of different Ag-O_I values due to second-order Jahn-Teller effects was not considered. In the case of the cluster with twelve water molecules two discrete shells were formed (4 H₂O first shell and 8 H₂O second shell). The large number of geometrical parameters in [Ag(H₂O)₁₂]⁺ and, in particular, the lability of the force constants associated to the intermolecular dihedral and bond angles, compelled us to relax the optimization criteria with respect to the usual threshold: a full optimization was undertaken up to energy changes lower than 10⁻⁵ au at the RHF level; afterwards only both Ag-O_I and Ag-O_{II} distances were optimized at the MP2 level. For the calculation of this large cluster within the cavity, only the 12 Ag-O distances were optimized. The rest of geometrical parameters were kept at the gas phase values.

The average effect of the electrostatic interactions between the hydrate and the bulk solvent was taken into account by means of the self-consistent reaction field (SCRf) method developed by Nancy's group.³¹ The solute charge distribution is expanded as a series of electric multipole moments (in these computations the series was truncated at the sixth order) placed in a constant coordinate cavity (in our case was spherical or ellipsoidal depending on the cluster symmetry) surrounded by a polarizable continuum dielectric (which was set up to the static dielectric permittivity of water, 78.39). Efficient geometry optimization procedures have recently been implemented based on analytical definition of the solvation energy gradient, allowing the use of a deformable cavity, which adapts to the solute geometry during the search process of its optimum structure.³² The cavity volumes were obtained by means of the accessible molecular surface method³³ as implemented in GEPOL92 program.³⁴ The standard use of a cavity for the supermolecule obtained from the simple addition of the molecular volumes of the monomers is not valid since some limited regions of space external to monomer surfaces are not accessible to the solvent molecules,^{13,35} and they should be better considered belonging to the supermolecule ensemble than to the solvent. Cavity volumes used have been included in Table 1. Computations have been carried out with the GAUSSIAN-94 program³⁶ and a set of independent links³⁷ which implements the Nancy's solvation model up to the MP2 level.^{20,38}

3. Results and Discussion

The main optimized geometrical parameters at the MP2 level for all the clusters in gas phase and in solution ($\epsilon = 78.39$) have been included in Table 1. Considering the changes in the parameters for the different [Ag(H₂O)_{*n*}]⁺ clusters in gas phase, one notices that the main change is associated with the Ag-O distance. Within the first hydration shell, *R*(Ag-O_I) increases with the number of water molecules in this shell (2.291 Å for *n* = 1 and 2.433 Å for *n* = 4). For the dimer a shortening is observed due to the covalent component of this bond; the OAgO angle in solution is 130° and this arrangement is not yet affected by the water-water repulsions. When the second hydration

TABLE 1: MP2 Optimized Geometrical Parameters for $[\text{Ag}(\text{H}_2\text{O}_n)^+]$ Clusters in Vacuum and in Solution, and the Cavity Volume for the Optimized Geometry^a

<i>n</i>	gas phase					solution ($\epsilon = 78.39$)			
	<i>R</i> (Ag–O)	<i>R</i> (Ag–H)	<i>R</i> (O–H)	\angle HOH	θ	<i>R</i> (Ag–O)	<i>R</i> (Ag–H)	θ	<i>V</i> _{cavity}
1	2.291	2.982	0.973	105.5	0	2.369	2.952	40.1	74.4
2	2.258	2.947	0.972	105.9	0	2.353	2.977	31.9	142.3
4	2.433	3.120	0.971	104.9	1.8	2.460	3.170	15.7	376.5
12 first shell (4)	2.400	3.08 ^b	0.972	105.9	2.5 ^b	2.430	3.11 ^b	2.5	1250.9
second shell (8)	4.70 ^b	5.28 ^b	0.971	105.0		4.76 ^b	5.34 ^b		

^a Bond lengths in Å, angles in deg, and volumes in Å³. ^b Average value

shell is added to the tetrahydrate, this distance reduces to 2.400 Å. This result agrees with previous theoretical studies where a partial second shell of water molecules was considered.^{9,11} Likewise, intramolecular parameters of water molecules change slightly with the specific interactions since an isolated water molecule has a value of 0.969 Å for *R*(O–H) and 103.4° for the HOH angle. A slight increase in the O–H bond and in the bond angle with the presence of a second shell of water molecules had already been observed by other authors.^{11,39} If geometrical relaxation of these clusters in the presence of a polarizable continuum is considered, the Ag–O distances increase, in particular the Ag–O_I one, as we had already observed for other hydrates of multivalent cations.¹² *R*(Ag–O_I) increases about 0.08 Å for the monomer and dimer, and 0.03 Å for the $[\text{Ag}(\text{H}_2\text{O})_4]^+$ and $[\text{Ag}(\text{H}_2\text{O})_{12}]^+$ clusters. *R*(Ag–O_{II}) in the $[\text{Ag}(\text{H}_2\text{O})_{12}]^+$ cluster lengthens about 0.06 Å. As expected, the distortion effect on the second hydration shell is larger than on the first one.

When one considers the combined effect of the specific interactions of a second hydration shell, mainly the hydrogen bonding, and the long-range interactions due to the bulk solvent on the Ag⁺ tetrahydrate, a cancellation of both effects is found. The Ag–O_I distance is 2.43 Å in gas phase as well as with the whole solvation model, i.e., $[\text{Ag}(\text{H}_2\text{O})_{12}]^+$ in the cavity. The Ag–H_I distances whose values are 3.12 Å for the tetrahydrate in gas phase reduce to 3.11 Å when the whole model is used. However, when more incomplete solvent representations are used, that is, the two discrete shell model, $[\text{Ag}(\text{H}_2\text{O})_{12}]^+$, or the $[\text{Ag}(\text{H}_2\text{O})_4]^+$ within the cavity, the Ag–O_I and Ag–H_I distances are less similar to the values of the whole model than to those of gas phase, i.e., 2.40 and 2.46 Å, and 3.08 and 3.17 Å, respectively.

One of the points stressed by Tuñón et al.¹³ and Akkeson et al.¹⁴ is that the cavity size is crucial in determining the cation–oxygen distance within a mixed discrete-continuum model. Thus, a larger volume could be responsible for the lengthening of the intermolecular distances, while smaller cavities should favor the opposite geometrical trend given that for charged systems the Born solvation term (monopole) highly increases with the diminution of the effective cavity radius. To clarify this point, we have performed an additional geometry optimization of the $[\text{Ag}(\text{H}_2\text{O})]^+$ cluster within a cavity whose volume was reduced to 90% of that used in Table 1. The Ag–O distance increases by 0.02 Å and the tilt angle θ by 3°, compared to the values shown in Table 1 for this monohydrate in solution. The basic requirement of the good convergence for the multipolar expansion of the solute–solvent interaction energies was fulfilled in all cases. Therefore, when reducing the cavity size the trend observed with the continuum is reinforced. This can be understood by realizing that when the cavity volume is reduced, solvent reaction field effects become greater, and the structure of the monohydrate relaxes such that the multipolar contributions to the interaction energy increase. The reduction of the Ag–O_I distance to favor a decrease of the Born term (a consequence of the reduction in the cavity volume) does not take place, since the energetic cost associated to the shrinkage

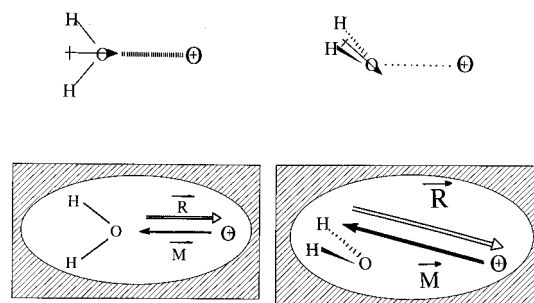


Figure 2. Qualitative representation of the ion–water dielectric interaction in terms of electric moments in gas (top) and condensed (bottom) phase as a function of the tilt water angle. *M* represents the global electric moment of the ion–water ensemble and *R* represents the solvent reaction field.

of the monomer cannot be compensated. In other words, the force constant coupled to the Ag–O bond is stronger than that associated to the Born solvation term.

One striking finding arising from Table 1 concerns the tilt water angle θ , which has a noticeable value in solution for the small clusters. It has long been observed by X-ray neutron diffraction that the M–O_I and M–H_I distances are such that the water molecular plane does not contain the metal cation; i.e., there is a tilt angle θ , differing from zero, being particularly important for monovalent and large cations.⁵ Quantum-mechanical calculations of isolated hydrates do not account for tilt angle. When these clusters are considered in the gas phase, the main intermolecular interaction is the ion–dipole one which is favored by a planar arrangement. Metal–oxygen bonds containing specific orbital interactions are discarded from this purely electrostatic reasoning line. The final geometry of the supermolecule within a cavity will be a compromise between the intermolecular ion–water interactions and the supermolecule-polarized continuum ones. The total dipolar and quadrupolar components of the monohydrate (supermolecule) increases with the increase of the tilt angle, and these stabilizing solute–solvent reaction field interactions are more important than the intracavity ion–dipole water ones. Figure 2 gives a qualitative scheme of this interpretation. Therefore, the cavity model is able to predict the appearance of the tilt angle. Figure 3 shows the energy profile along the tilt angle for $[\text{Ag}(\text{H}_2\text{O})]^+$ in gas phase and solution. One can observe that for gas phase there is a defined well centered at 0°, but for the monohydrate in cavity, the energy profile highly changes showing a minimum at ~40°. The height of the interconversion barrier is lower than the *kT* value at room temperature. Thus, this geometrical parameter becomes then almost free at room temperature, although the minimum obtained should contribute to the tilt angle observed.⁴⁰ Sandström et al.²⁷ determine a 45° tilt angle in $\text{Ag}(\text{ClO}_4)$ aqueous solutions. It is worth pointing out that the tilt angle reduces when larger polyhydrates are considered, in our opinion, due to the implicit symmetry which is introduced when completing the first and second hydration shells. Likewise, other factors which are not considered in our modelization

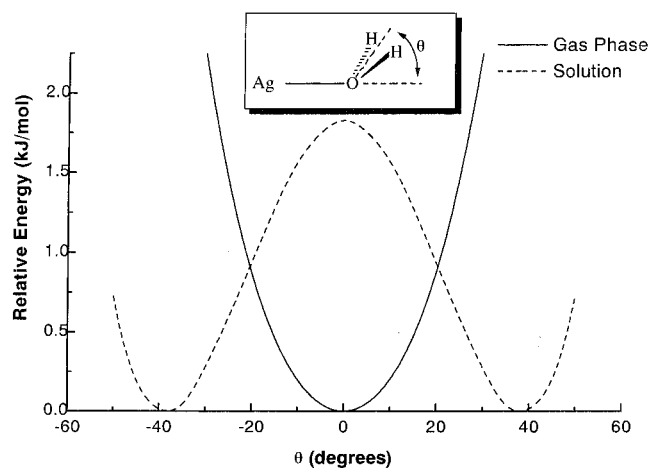


Figure 3. Energy (kJ/mol) vs tilt angle θ (deg) for the $\text{Ag}(\text{H}_2\text{O})_n^+$ in gas phase and in solution ($\epsilon = 78.39$).

such as outer-sphere ion-pair formation in concentrated solution can contribute to the observed water tilt angle.⁶

Seward et al.⁴¹ have recently studied by EXAFS the hydration of Ag^+ in hydrothermal solutions from 25 to 350 °C and have observed a decrease of the $\text{Ag}-\text{O}_I$ bond length when passing from room temperature to 350 °C. These authors point out that based on previous high-temperature EXAFS measurements on other ions such as Sr^{2+} , Cd^{2+} , In^{3+} , and Rb^+ ,^{41,42,43} the first shell contraction of hydrated cations with increasing temperature is a fundamental property. Among the possible phenomena responsible of this shortening in the $\text{M}-\text{O}_I$ distance the large decrease of the dielectric permittivity of the medium with the temperature⁴⁴ should be invoked as a fundamental factor. The results obtained by the use of the continuum model in our previous work on multivalent hydrated cations¹² and those presented here on the silver cation seem to give theoretical support to Seward et al.'s findings. Thus, we have shown that the presence of a dielectric continuum leads to a systematic lengthening of the cation–oxygen distance, and consequently, the previous distance reduces when thermal effects lead to a decrease of dielectric properties. It is worth mentioning that, if the local hydrogen bonding structure around Ag^+ was mainly responsible for the $\text{Ag}-\text{O}_I$ distance, when the temperature increased an opposite effect on the distance would have been observed, i.e., a lengthening. Therefore, it seems that this temperature-dependent property is caused by a global and long-range behavior of the solvent. Another factor invoked by Seward et al. to explain the shortening of this distance concerns the large kinetic energy of solvent molecules associated with high temperature of solution. Collisions of these molecules with hydrate would allow a closer approach of water molecules to the cation. Nevertheless, according to previous results⁴⁵ on deformation of $[\text{Zn}(\text{H}_2\text{O})_6]^{2+}$, the energetic cost of this hydrate shrinking is much greater than the transferred energy involved in the collision.

The main experimental distances of silver salt aqueous solutions are 2.32–2.43 Å for the $\text{Ag}-\text{O}_I$, 2.97–3.1 Å for the $\text{Ag}-\text{H}_I$,^{27,46} and 2.9 Å for the O_I-O_{II} ,⁴⁷ and also evidence for a second shell of water molecules with $\text{Ag}-\text{O}_{II}$ in the range 4–5 Å has been given.²⁷ From Table 1 it is concluded that theoretical distances are largely similar to the experimental ones within the error bars. (Although not shown in Table 1, $R(\text{O}_I-\text{O}_{II})$ for the cluster with $n = 12$ in solution is 2.89 Å.) This agreement is quite satisfactory even at the quantitative level.

Paradoxically, the more complete solvation model of three shells (two hydration shells + continuum) predicts almost the same $\text{Ag}-\text{O}_I$ and $\text{Ag}-\text{H}_I$ distances as those obtained in the case of the tetrahydrate in gas phase. This represents an example

TABLE 2: Solvation Enthalpy for the Different $[\text{Ag}(\text{H}_2\text{O})_n]^+$ Clusters and Its Components within the Semicontinuum Model of Solvation (in kJ/mol)

n	ΔH_{hydr}	ΔH_{sup}	ΔH_{cont}	ΔH_{cav}	$\Delta H_{\text{disp-rep}}$	$n\Delta H_{\text{vap}}(\text{H}_2\text{O})$
1	-383.0	-117.5	-294.8	5.0	-17.5	41.8
2	-407.2	-225.9	-241.4	6.9	-30.5	83.7
4	-411.1	-345.5	-190.9	10.8	-52.9	167.4
12	-342.6	-592.0	-145.0	26.3	-134.0	502.1

of the fortuitous agreement which may be found when hydrate structures are calculated in gas phase and compared with the experimental values obtained in solution due, at least in part, to the mutual cancellation between specific and long range solute–solvent interactions.

Table 2 gives the predicted Ag^+ hydration energy for the different polyhydrates calculated within the semicontinuum model of solvation,¹⁸ adapted to the particular case of the ion solvation.^{12,48} On this basis, the hydration enthalpy is calculated by the expression

$$\Delta H_{\text{hydr}} = \Delta H_{\text{sup}} + \Delta H_{\text{cont}} + \Delta H_{\text{cav}} + \Delta H_{\text{disp-rep}} + n\Delta H_{\text{vap}}$$

where ΔH_{sup} is the formation enthalpy of the cluster, which is calculated from the difference between the gas phase ab initio energies of each cluster and its components, including ZPE, thermal corrections, and the term ΔnRT to deal with the enthalpy magnitude; ΔH_{cont} is the solvation energy corresponding to the long-range interactions of the hydrated cluster embedded in a cavity with a dielectric continuum of $\epsilon = 78.39$, the entropic contribution to the solvation free energy has been subtracted according to the procedure given by Tomasi et al. elsewhere;⁴⁹ ΔH_{cav} is the enthalpy needed to create the cavity inside the continuum, which is calculated by means of Pierotti's formula;⁵⁰ $\Delta H_{\text{disp-rep}}$ is the hydrate-continuum dispersion contribution which is calculated by the method of Tomasi et al.,^{49,51} and $n\Delta H_{\text{vap}}$ is the enthalpy needed to bring n water molecules from the liquid pure solvent to the gas phase, in order to form the cluster (the experimental value of water vaporization enthalpy, -41.8 kJ/mol has been used). The Ag^+ hydration enthalpy predicted for the different clusters suggests that calculations derived from the three-shell model, i.e., results for $n = 12$ in the continuum, are not satisfactory; the error in the estimation of this magnitude is about 130 kJ/mol. This seems to indicate that the usual scheme to calculate the solvation energy based on the semicontinuum approach does not work when more than one solvation shell is explicitly considered. Evaluation of ΔH_{sup} implies the calculation of differences among absolute energies that are always affected by uncertainties which increase with the number of water molecules; in other words, this magnitude is an error source for ΔH_{hydr} that increases with the size of the hydrate. The application of statistical formulas to convert energies to enthalpies for large supermolecules may be as well an error source. In this sense, it seems that these factors can be more efficiently treated by means of statistical methods.⁵² A second point is the small difference observed between the hydration energy, ΔH_{hydr} , obtained for the dimer and the tetramer, which in fact does not allow an energetic discrimination of the coordination number based on this criteria, as have been previously shown for other multivalent cations by Tomasi et al.⁴⁸ and by us.¹² Moreover, the error in estimating the Ag^+ hydration enthalpy ($\Delta H_{\text{hydr}}(\text{exptl}) = -474$ kJ/mol) is of the same order as that found for other multivalent cations,^{12,48} ~60 kJ/mol, although due to the small absolute value for this monovalent cation, the relative error is increased by a factor of 3. Given the number of contributions to ΔH_{hydr} , it is a difficult task to point out the larger source of this discrepancy.

In contrast, the ΔG_{hydr} estimation for Li^+ hydration calculated by Tomasi et al.⁴⁸ on the basis of the tetrahydrated cation, with

a similar model to that employed here, is -484.9 kJ/mol, the experimental one being -489 kJ/mol. We have performed an estimation of the Li^+ hydration enthalpy from the $[\text{Li}(\text{H}_2\text{O})_4]^+$ following the same methodology used for the Ag^+ case. DZP basis sets were chosen for Li. $\text{Li}-\text{O}_1$ distance was found to be 1.99 \AA and the cavity volume was 242.4 \AA^3 . The result is $\Delta H_{\text{hydr}} = -533.8$ kJ/mol ($\Delta H_{\text{sup}} = -440.9$, $\Delta H_{\text{cont}} = -212.0$; $\Delta H_{\text{cav}} = 9.8$, $\Delta H_{\text{disp-rep}} = -48.11$, and $n\Delta H_{\text{vap}}(\text{H}_2\text{O}) = 167.4$ kJ/mol) which is quite close to the experimental value of -520 kJ/mol. This seems to indicate that the evaluation of the hydration energies for Ag^+ , a larger and softer monovalent cation than Li^+ , is less accurate. In our opinion, a significant part of this discrepancy between the employed model and the experimental phenomenon lies in the dispersion contribution beyond the first hydration shell. Therefore, we conclude that the simplicity of the model which represents the solvation process guarantees a degree of confidence in the estimation of solvation energy of cations that appear to be less accurate when less electrostatic components are involved.

This work presents a combined solvation model where the solute-solvent specific and continuum interactions have been considered quantum-mechanically. At first sight, one may conclude that for a highly structured and polar solvent as water, a good representation could be attained by placing several solvation shells within a cavity immersed in a continuum to fulfill the electrostatic requirements of the solvent as dielectric. However, the results suggest that these requirements contrast with the difficulty in the quantum-mechanical treatment of a large number of particles weakly bounded. Thus a compromise should be found between the simplicity of the system and the accuracy of the required data. It is clear that for detailed descriptions of the charged solute and its local environment, a quantum-mechanical methodology has to be employed. But, its generalization to a quantum solvent model which is completely discrete seems to present a deeper and intrinsic limitation than the computational cost: the physics of the condensed medium cannot be well represented without including statistical factors. From this, strategies such as the semicontinuum approach or hybrid quantum mechanics/classical mechanics techniques are revealed as useful tools in the understanding of the solvation phenomenon.

Acknowledgment. We thank the Spanish Dirección General de Investigación Científica y Técnica for financial support (PB95-0549). J.M.M. and R.R.P. acknowledge the Ministerio de Educación of Spain for a doctoral fellowship and a post-doctoral contract, respectively.

References and Notes

- Burgess, J. *Ions in Solution*; Ellis Horwood: Chichester, U.K., 1988.
- Rosen, M. J. *Surfactants and Interfacial Phenomena*; Wiley-Interscience: New York, 1978.
- Marcus, Y. *Ion Solvation*; Wiley: Chichester, U.K., 1986.
- Marcus, Y. *Chem. Rev.* **1988**, *88*, 1475.
- Ohtaki, H.; Radnai, T. *Chem. Rev.* **1993**, *93*, 1157.
- Magini, M.; Licheri, G.; Paschina, G.; Piccaluga, G.; Pinna, G. *X-Ray Diffraction of Ions in Aqueous Solutions: Hydration and Complex Formation*; CRC Press: Boca Raton, FL, 1988.
- Clementi, E.; Corongiu, G.; Aida, M.; Nieser, U.; Kneller, G. In *MOTEC-90: Modern Techniques in Computational Chemistry*; Clementi, E., Ed.; ESCOM: Leiden, The Netherlands, 1990; Chapter 17.
- Tapia, O. In *Theoretical Models of Chemical Bonding*; Maksic, Z. B., Ed.; Springer-Verlag: Berlin, 1991; Vol. 4, pp 435-458.
- Mhin, B. J.; Lee, S.; Cho, S. J.; Lee, K.; Kim, K. S. *Chem. Phys. Lett.* **1992**, *197*, 77. Lee, S.; Kim, J.; Park, J. K.; Kim, K. S. *J. Phys. Chem.* **1996**, *100*, 14329.
- Akesson, R.; Pettersson, L. G. M.; Sandström, M.; Wahlgren, U. *J. Phys. Chem.* **1992**, *96*, 150.
- Katz, A. K.; Glusker, J. P.; Beebe, S. A.; Bock, C. W. *J. Am. Chem. Soc.* **1996**, *118*, 5752. Bock, C. W.; Katz, A. K.; Glusker, J. P. *J. Am. Chem. Soc.* **1995**, *117*, 3754.
- Sánchez Marcos, E.; Pappalardo, R. R.; Rinaldi, D. *J. Phys. Chem.* **1991**, *95*, 8928.
- Tuñón, I.; Silla, E.; J. Bertrán, J. *J. Phys. Chem.* **1993**, *97*, 5547.
- Akesson, R.; Pettersson, L. G. M.; Sandström, M.; Siegbahn, P. E. M.; Wahlgren, U. *J. Phys. Chem.* **1992**, *96*, 10773.
- Karlström, G. *J. Phys. Chem.* **1988**, *92*, 1318.
- Bertrán, J.; Ruíz-López, M. F.; Rinaldi, D.; Rivail, J. L. *Theor. Chim. Acta* **1992**, *84*, 181.
- Reichardt, C. *Solvents and Solvent Effects in Organic Chemistry*, 2nd Ed.; VCH: Weinheim, FRG, 1990.
- Tomasi, J.; Persico, M. *Chem. Rev.* **1994**, *94*, 2027.
- Cramer, C. J.; Truhlar, D. G. In *Reviews in Computational Chemistry*; Lipkowitz, K. B., Boyd, D. B., Eds.; VCH Publishers: New York, 1995; Vol. 6, pp 1-72.
- Rivail, J. L.; Rinaldi, D. In *Computational Chemistry, Reviews of Current Trends*; Leszczynski, J., Ed.; World Scientific: New York, 1996; Chapter 4.
- Allen, M. P.; Tildesley, D. J. *Computer Simulation of Liquids*; Clarendon Press: Oxford, U.K., 1989; pp 155-166.
- Elrod, M. J.; Saykally, R. J. *Chem. Rev.* **1994**, *94*, 1975.
- Roberts, J. F.; Schnitker, J. *J. Chem. Phys.* **1994**, *101*, 5024.
- Gao, J. In *Reviews in Computational Chemistry*; Lipkowitz, K. B., Boyd, D. B., Eds.; VCH Publishers: New York, 1996; pp 119-187.
- Akesson, R.; Pettersson, L. G. M.; Sandström, M.; Wahlgren, U. *J. Am. Chem. Soc.* **1994**, *116*, 8691.
- Texter, J.; Hastreiter, J. J.; Hall, J. L. *J. Phys. Chem.* **1983**, *87*, 4690.
- Sandström, M.; Neilson, G. W.; Johansson, G.; Yamaguchi, T. *J. Phys. C: Solid State Phys.* **1985**, *18*, L1115.
- Stevens, W. J.; Basch, H.; Krauss, J. *J. Chem. Phys.* **1984**, *81*, 6026.
- Stevens, W. J.; Basch, H.; Krauss, J. *Can. J. Chem.* **1992**, *70*, 612.
- Szalewicz, K.; Cole, S. J.; Kolos, W.; Bartlett, R. J. *J. Chem. Phys.* **1988**, *89*, 3662.
- Langhoff, S. R.; Pettersson, L. G. M.; Bauschlicher, C. W. Jr.; Partridge, H. *J. Chem. Phys.* **1987**, *86*, 268.
- Rivail, J. L.; Rinaldi, D. *Chem. Phys.* **1976**, *18*, 233. Rinaldi, D.; Ruíz-López, M. F.; Rivail, J. L. *J. Chem. Phys.* **1983**, *78*, 834.
- Rinaldi, D.; Rivail, J. L.; Rguini, N. *J. Comput. Chem.* **1992**, *13*, 675.
- Lee, B.; Richards, F. M. *J. Mol. Biol.* **1971**, *55*, 379.
- Silla, E.; Tuñón, I.; Pascual-Ahuir, J. L. *J. Comput. Chem.* **1991**, *12*, 1077. Pascual-Ahuir, J. L.; Silla, E.; Tuñón, I. *QCPE Bull.* **1992**, *12*, 63. QCPE program 554.
- Pappalardo, R. R.; Sánchez Marcos, E. *J. Chem. Soc., Faraday Trans.* **1991**, *87*, 1719.
- Gaussian 92* (Revision B.3); Frisch, M. J.; Trucks, G. W.; Schlegel, H. B.; Gill, P. M. W.; Johnson, B. G.; Robb, M. A.; Cheeseman, J. R.; Keith, T. A.; Petersson, G. A.; Montgomery, J. A.; Raghavachari, K.; Al-Laham, M. A.; Zakrzewski, V. G.; Ortiz, J. V.; Foresman, J. B.; Cioslowski, J.; Stefanov, B. B.; Nanayakkara, A.; Challacombe, M.; Peng, C. Y.; Ayala, P. Y.; Chen, W.; Wong, M. W.; Andres, J. L.; Replogle, E. S.; Gomperts, R.; Martin, R. L.; Fox, D. J.; Binkley, J. S.; Defrees, D. J.; Baker, J.; Stewart, J. P.; Head-Gordon, M.; Gonzalez, C.; Pople, J. A. *Gaussian, Inc.*: Pittsburgh, PA, 1995.
- Rinaldi, D.; Pappalardo, R. R. *SCRFPAC, QCPE Bull.* **1992**, *12*, 69. QCPE program 662.
- Rivail, J. L. *C.R. Acad. Sc. Paris*, **1990**, *307*, 311.
- Probst, M. M.; Hermansson, K. *J. Chem. Phys.* **1992**, *96*, 8995.
- Enderby, J. E. *Chem. Soc. Rev.* **1995**, 159.
- Seward, T. M.; Henderson, C. M. B.; Charnock, J. M.; Dobson, B. R. *Geochim. Cosmochim. Acta* **1996**, *60*, 2273.
- Seward, T. M.; Henderson, C. M. B.; Charnock, J. M.; Dobson, B. R. *Water-Rock Interaction* **1995**, *8*, 43.
- Palmer, B. J.; Pfund, D. M.; Fulton, J. L. *J. Phys. Chem.* **1996**, *100*, 13393.
- Tödheide, K. In *Water. A Comprehensive Treatise*; Franks, F., Ed.; Plenum Press: New York, 1972; Chapter 13.
- Sánchez Marcos, E.; Martínez, J. M.; Pappalardo, R. R. *J. Chem. Phys.* **1996**, *105*, 5968.
- Ichikawa, T.; Li, A. S. W.; Kevan, L. *J. Chem. Phys.* **1981**, *75*, 2472.
- Yagamuchi, T.; Johansson, G.; Holmberg, B.; Maeda, M.; Ohtaki, H. *Acta Chem. Scand. A* **1984**, *38*, 437.
- Floris, F.; Persico, M.; Tani, A.; Tomasi, J. *Chem. Phys.* **1995**, *195*, 207.
- Bonaccorsi, R.; Palla, P.; Tomasi, J. *J. Am. Chem. Soc.* **1984**, *106*, 1945.
- Pierotti, R. A. *Chem. Rev.* **1976**, *76*, 715.
- Floris, F.; Tomasi, J. *J. Comput. Chem.* **1989**, *10*, 616. Floris, F.; Tomasi, J.; Pascual-Ahuir, J. L. *J. Comput. Chem.* **1991**, *12*, 784.
- Pappalardo, R. R.; Sánchez Marcos, E. *J. Phys. Chem.* **1993**, *97*, 4500. Pappalardo, R. R.; Martínez, J. M.; Sánchez Marcos, E. *J. Phys. Chem.* **1996**, *100*, 11748.